Lynx X-Ray Observatory: an overview

Jessica A. Gaskin
Douglas A. Swartz
Alexey Vikhlinin
Feryal Özel
Karen E. Gelmis
Jonathan W. Arenberg
Simon R. Bandler
Mark W. Bautz
Marta M. Civitani
Alexandra Dominguez
Megan E. Eckart
Abraham D. Falcone
Enectali Figueroa-Feliciano
Mark D. Freeman
Hans M. Günther
Keith A. Havey

Ralf K. Heilmann
Kiranmayee Kilaru
Ralph P. Kraft
Kevin S. McCarley
Randall L. McEntaffer
Giovanni Pareschi
William Purcell
Paul B. Reid
Mark L. Schattenburg
Daniel A. Schwartz
Eric D. Schwartz
Harvey D. Tananbaum
Grant R. Tremblay
William W. Zhang
John A. Zuhone

SPIE.

Lynx X-Ray Observatory: an overview

Jessica A. Gaskin,[a,*] **Douglas A. Swartz,**[b] **Alexey Vikhlinin,**[c] **Feryal Özel,**[d] **Karen E. Gelmis,**[a] **Jonathan W. Arenberg,**[e] **Simon R. Bandler,**[f] **Mark W. Bautz,**[g] **Marta M. Civitani,**[h] **Alexandra Dominguez,**[a] **Megan E. Eckart,**[i] **Abraham D. Falcone,**[j] **Enectali Figueroa-Feliciano,**[k] **Mark D. Freeman,**[c] **Hans M. Günther,**[g] **Keith A. Havey,**[l] **Ralf K. Heilmann,**[g] **Kiranmayee Kilaru,**[b] **Ralph P. Kraft,**[c] **Kevin S. McCarley,**[a] **Randall L. McEntaffer,**[j] **Giovanni Pareschi,**[h] **William Purcell,**[m] **Paul B. Reid,**[c] **Mark L. Schattenburg,**[g] **Daniel A. Schwartz,**[c] **Eric D. Schwartz,**[c] **Harvey D. Tananbaum,**[c] **Grant R. Tremblay,**[c] **William W. Zhang,**[f] **and John A. Zuhone**[c]

[a]NASA Marshall Space Flight Center, Huntsville, Alabama, United States
[b]Universities Space Research Association, Huntsville, Alabama, United States
[c]Smithsonian Astrophysical Observatory, Cambridge, Massachusetts, United States
[d]University of Arizona, Tucson, Arizona, United States
[e]Northrop Grumman, Aerospace Systems, Redondo Beach, California, United States
[f]NASA Goddard Space Flight Center, Greenbelt, Maryland, United States
[g]MIT Kavli Institute for Astrophysics and Space Research, Cambridge, Massachusetts, United States
[h]Osservatorio Astronomico di Brera, Merate, Lecco, Italy
[i]Lawrence Livermore National Laboratory, Livermore, California, United States
[j]Pennsylvania State University, University Park, Pennsylvania, United States
[k]Northwestern University, Evanston, Illinois, United States
[l]Harris Corporation Space and Intelligence Systems, Rochester, New York, United States
[m]Ball Aerospace and Technologies Corporation, Boulder, Colorado, United States

Abstract. Lynx, one of the four strategic mission concepts under study for the 2020 Astrophysics Decadal Survey, provides leaps in capability over previous and planned x-ray missions and provides synergistic observations in the 2030s to a multitude of space- and ground-based observatories across all wavelengths. Lynx provides orders of magnitude improvement in sensitivity, on-axis subarcsecond imaging with arcsecond angular resolution over a large field of view, and high-resolution spectroscopy for point-like and extended sources in the 0.2- to 10-keV range. The Lynx architecture enables a broad range of unique and compelling science to be carried out mainly through a General Observer Program. This program is envisioned to include detecting the very first seed black holes, revealing the high-energy drivers of galaxy formation and evolution, and characterizing the mechanisms that govern stellar evolution and stellar ecosystems. The Lynx optics and science instruments are carefully designed to optimize the science capability and, when combined, form an exciting architecture that utilizes relatively mature technologies for a cost that is compatible with the projected NASA Astrophysics budget. © *The Authors. Published by SPIE under a Creative Commons Attribution 4.0 Unported License. Distribution or reproduction of this work in whole or in part requires full attribution of the original publication, including its DOI.* [DOI: 10.1117/1.JATIS.5.2.021001]

1 Introduction

In 2016, four large strategic mission concepts, based on those defined in the Astrophysics Roadmap—Enduring Quests, Daring Visions,[1] were selected by the astronomy community to be studied for prioritization in the 2020 Astrophysics Decadal Survey. Of these missions, Lynx, formerly x-ray surveyor, is the only concept that will enable the next generation of high-energy observations of the Universe, impacting all areas of astronomy. Since being selected for study, the Lynx concept has evolved into a streamlined observatory capable of performing revolutionary science befitting that of a flagship mission for a cost that permits a balanced Astrophysics portfolio. This paper overviews the Lynx payload, observatory architecture, and major mission elements, providing context for the specific technology papers that are highlighted in this paper. The development of the Lynx X-Ray Observatory concept is made possible through the multitude of contributions from the Science and Technology Definition Team (STDT), Science and

Instrument Working Group members, X-ray Optics Working Group and Development teams, Marshall Space Flight Center (MSFC) Advanced Concept Office, and Goddard Space Flight Center (GSFC) concept design teams, the Jet Propulsion Laboratory (JPL), industry partners, and the general astronomy community. The Lynx Study Office supports and manages the study and is a partnership between MSFC and the Smithsonian Astrophysical Observatory (SAO). This partnership capitalizes on the decades-long relationship between the two institutions to support the Chandra X-Ray Observatory.

1.1 Fascinating Observations

Rooted in the x-ray band, Lynx will operate in the 0.2-to ~10-keV energy range and boasts a ~100-fold increase in sensitivity compared with the currently orbiting Chandra X-Ray Observatory. This increase in sensitivity is achieved by coupling Chandra-like angular resolution with significantly increased throughput. Lynx will also have 16 times larger field of view (FOV) for subarcsecond imaging and 10 to 20 times higher spectral resolution for both point-like and extended sources. These attributes are highlighted in Fig. 1.

*Address all correspondence to Jessica A. Gaskin, E-mail: jessica.gaskin@nasa.gov
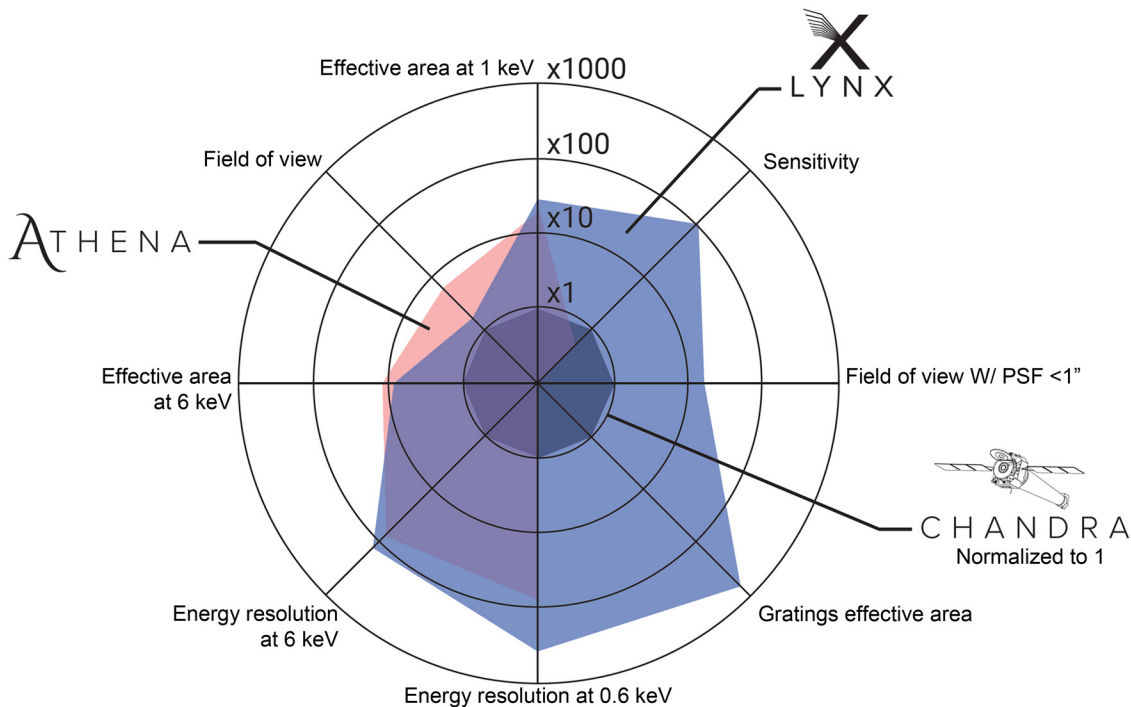
Fig. 1 Lynx will be the most capable x-ray observatory built, with significant increases in sensitivity, FOV with subarcsecond imaging, and spectral resolution over Chandra and ATHENA. The sensitivity axis is the inverse of the flux threshold achievable in 4 Ms surveys in the 0.5- to 2-keV energy band, for identical levels of the false detection probability (e.g., 4.5 sigma). Lynx will also provide high-resolution imaging spectroscopy in the form of an x-ray microcalorimeter. This x-ray microcalorimeter will be unique in that it will be able to provide arcsecond imaging—a crucial capability for accomplishing Lynx science goals, such as exposing the physics of energy feedback shaping the evolution of galaxies.

The majority of Lynx science will be performed through a General Observer (GO) Program, enabling a broad range of compelling discovery science and exploration, most of which is only accessible at high energies. The Lynx architecture was designed to enable even the most challenging of these observations, such as discerning the first supermassive black holes at high redshift ($z = 10$), and mapping the hot tenuous gas around galaxies and in the Cosmic Web that is critical to galaxy formation and evolution. More specifically, the Lynx architecture flows directly from the science requirements established by the STDT and supported by a large number of community Science Working Group members. These science requirements are encapsulated within the Lynx science pillars, summarized below. A more detailed discussion of the Lynx science can be found in the Lynx 2018 Interim Report[2] and in the Final Report to the Decadal Committee, which is currently in preparation.[3]

The dawn of black holes. Massive black holes start to form as early as their host galaxies. Lynx will find the first supermassive black holes in the first galaxies detected by JWST, trace their growth from the seed phase, and shed light on how they subsequently co-evolve with the host galaxies. Reaching into the seed regime in the early Universe requires x-ray sensitivities of $\sim 10^{-19}$ erg s^{-1} cm^{-2}. These observations require Lynx to have a large effective area of around 2 m^2 at 1 keV, and large FOV with subarcsecond or better angular resolution. Lynx's high-angular resolution will allow every Lynx-detected x-ray source to be uniquely associated with a JWST-detected galaxy by eliminating source-confusion at these high redshifts. Further,

Lynx will provide a census of black hole growth throughout cosmic time to answer fundamental questions such as "How are supermassive black holes connected to their host galaxies?" "Do all supermassive black holes emerge at high redshifts?" "Can relics of the black hole seeds be found in nearby galaxies?"

The invisible drivers of galaxy formation and evolution. The assembly, growth, and state of the visible matter in cosmic structures are largely driven by violent processes that produce and disperse large amounts of energy and metals into the surrounding medium. In galaxies at least as massive as the Milky Way, the relevant baryonic component is heated and ionized to x-ray temperatures. Lynx will be capable of mapping this hot gas around galaxies and in the Cosmic Web at high-angular resolution, allowing for the removal of contaminating point sources as well as characterizing in detail all significant modes of energy feedback. Essential observations require high-resolution spectroscopy ($R \sim 5000$) of background active galactic nuclei (AGNs), the ability to detect low-surface brightness continuum emission, and $R \sim 2000$ spectroscopy of extended sources on arcsecond scales. These capabilities are unique to Lynx.

The energetic side of stellar evolution and stellar ecosystems. Lynx will probe, to an unprecedented depth, a wide range of high-energy processes that provide a unique perspective on stellar birth and death, internal stellar structure, star–planet interactions, the origin of elements, and violent cosmic events. Lynx will detect x-ray emission as markers of young stars in active star forming regions, study stellar coronae in detail, and provide essential insight into the impact of stellar x-ray and extreme ultraviolet flux and winds on the habitability of their

planets. Images and spectra of supernova remnants (SNRs) in local group galaxies will extend studies of stellar explosions and their aftermath to different metallicity environments. Lynx will expand our knowledge of collapsed stars through sensitive studies of x-ray binaries in galaxies as distant as 10 Mpc and through detailed follow-ups of gravitational wave events. Lynx will greatly extend our x-ray grasp throughout the Milky Way and nearby galaxies by combining, for the first time, the required sensitivity, spectral resolution, and sharp vision to see in crowded fields.

1.2 Designing an Observatory

Lynx is able to achieve leaps in capability by coupling a lightweight, large area, high-resolution mirror assembly with good wide-field performance—0.5 arc sec half-power diameter (HPD) on-axis and better than 1 arc sec out to ~11 arc min radius—to a suite of three highly capable science instruments. This suite includes a large-scale active pixel sensor (APS) array, a high-resolution x-ray grating spectrometer (XGS), and an x-ray microcalorimeter.

All of the Lynx payload elements (mirrors and science instruments) have relatively mature candidate technologies and have well-defined paths for maturation within a decadal-driven timescale, lowering risk, and ultimately the cost of this mission. Multiple candidate technologies for the mirrors and the science instruments are described in detail in this paper. X-ray mirror technologies that were studied in detail by the Lynx team included silicon meta-shell optics developed by GSFC,[4] full-shell optics developed by Brera (INAF/Brera) and Marshall Spaceflight Center (MSFC),[5,6] and adjustable segmented optics developed by the SAO.[7,8] Similarly, multiple technologies were studied for the large-scale active sensor pixel array, dubbed the high-definition x-ray imager (HDXI)[9–12] and for the XGS.[13,14] The Lynx x-ray microcalorimeter (LXM)[15–21] is singular but has elements that have multiple candidate technologies. LXM also leverages heritage from Astro-H and Astro-E and design features from ATHENA.

1.3 Mission Architecture and Spacecraft Design Philosophy

The Lynx mission architecture and spacecraft design are intended to maximize science return while maintaining a straightforward design that could be implemented using existing processes and flight-hardware where possible. The Lynx mission and spacecraft elements borrow heavily from Chandra, the only x-ray observatory ever to achieve subarcsecond angular resolution.[22] Lynx maneuvers and operational procedures on-orbit are close to identical to Chandra's, and similar design approaches target longevity. Chandra's baseline mission was 5 years but has been operating for nearly 20 years and has maintained a robust science program throughout.[23] Similarly, Lynx will have a baseline mission lifetime of 5 years and will be provisioned for 20 years of operation. Operation beyond 20 years may be possible with the implementation of in-space servicing.[24]

By necessity, Lynx is a much more ambitious observatory (e.g., larger effective area and more advanced science instruments) than Chandra and will operate in a different environment (halo orbit around Sun–Earth L2 versus a highly elliptical orbit around the Earth). Lynx also takes advantage of many recent advances in the current state-of-the-art in the focal plane design,

propulsion systems, power system, avionics, command and data handling, and many other areas as appropriate.

Minimizing risk was also a factor in the mission and spacecraft design. To reduce risk, Lynx has been designed to not require any unique orbital or pointing maneuvers and complicated deployments. The number of on-board mechanisms related to the spacecraft has been minimized to include the solar array panels, which is a standard deployment on any space-based observatory, an outer door that will act as a sunshade, and an inner door that is used to reduce contamination during ground transport, integration, and in transit to orbit. There are a handful of additional mechanisms related to the payload as well that are discussed in Sec. 2.

1.4 State of Readiness

A preliminary program schedule for the Lynx has phase A starting in 2024, leading to a launch in the mid-2030s. Each of the Lynx payload technologies has elements that require maturation. A clear development path for reaching a technology readiness level (TRL) of 6 by the Project Preliminary Design Review in 2028 and for meeting Critical Design Review in 2030 has been defined for each of these enabling technologies in the Lynx technology roadmaps.[25] All of the Lynx enabling technologies are currently at a TRL of 3 or higher, and it is expected that all will be at or approaching a TRL 4 by the early 2020s. Each of these technologies is being funded through NASA competed opportunities or directed funding, internal institutional funding, and/or other preflight programs.

The Lynx schedule critical path is defined by the manufacturing of the many x-ray mirrors needed, regardless of mirror technology chosen for flight, to meet the required effective area. Steps will be taken to balance the cost, schedule, and risk associated with this schedule element. A cooperative agreement notice was awarded to a team of Northrop Grumman, Ball Aerospace, and Technologies Corporation, and Harris Corporation Space and Intelligence Systems to perform an independent cost, schedule, and risk assessment of the manufacturing aspects of x-ray mirrors considered by the Lynx concept study. This study task has resulted in an analytical model for the cost, schedule, and risk.[26] The theoretical foundation has been developed[27] and analysis has begun.[28]

2 Lynx X-Ray Observatory

The Lynx telescope design has a 3-m diameter mirror assembly with a 10-m focal length coupled to a suite of high-precision science instruments. This configuration allows for the science outlined in the Lynx science pillars to be completed within ~50% of the 5-year baseline mission. Lynx observations will primarily be made through a GO Program that not only includes Lynx architecture-defining pillar science but also includes additional critical science while still leaving time for as yet unimagined exploration. The astronomy community will further benefit from the operational observatory lifetime of 20 years without in-space servicing and even longer if one assumes servicing is available. Observatory longevity has purposefully been integrated into the observatory design to maximize the science return per mission cost. To accommodate the Lynx telescope, the observatory extends to 12.7-m in length and is 4.5-m in diameter at its largest point, which is the spacecraft bus (Fig. 2).

The Lynx observatory design includes the spacecraft bus, solar panels, support structure, and the Lynx telescope. Over
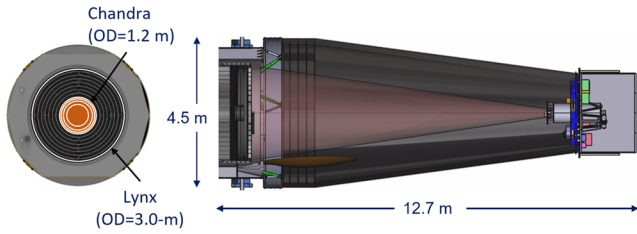
Fig. 2 The Lynx telescope has a mirror assembly that is 3-m in diameter, compared to that of Chandra's 1.2-m diameter mirror assembly, and a 10-m focal length. The Lynx spacecraft has been designed to accommodate the science-driven requirements while maintaining a simple, compact design that can be launched on multiple heavy-class and super-heavy-class vehicles (credit: NASA/M. Baysinger).

the past few years, the Lynx team has refined the design of all observatory elements with sufficiently high fidelity to propose a design reference mission (DRM) concept (Fig. 3). The increased science instrument fidelity is a result of multiple instrument design studies involving the Lynx Instrument Working Group and the instrument design labs at both NASA MSFC and GSFC. The Lynx mirror assembly (LMA) includes the x-ray mirror assembly (XMA), retractable x-ray grating array, and an AFT contamination cover. The contamination cover is used only on the ground to minimize contamination on the mirrors. Two of the science instruments, HDXI and the LXM, along with their electronics and radiators are mounted on a translation table that is part of integrated science instrument module (ISIM) so that either instrument can be placed in the focal position. A focus mechanism on the translation table allows for fine focus adjustment along the optical axis. The XGS focal plane detector assembly, called the XGD, is mounted in a fixed location on the ISIM offset from the optical axis to intercept the dispersed spectrum regardless of whether the HDXI or LXM is at the primary focus. The XGS focal plane assembly utilizes a separate focus mechanism that is integrated into its detector assembly housing.

2.1 X-Ray Mirror Assembly

Requirements for the XMA directly flow from the Lynx science goal to observe the first supermassive black hole seeds and unambiguously associate them with the first galaxies that JWST will observe.[29] Lynx's on-axis angular resolution of 0.5 arc sec (HPD) is required to avoid source confusion at the faintest fluxes and to uniquely associate x-ray sources with high-redshift optical and near-IR galaxies. A mirror effective area of 2 m^2 at 1 keV and an FOV with arcsecond or better imaging extending to ∼10 arc min off-axis would allow for the population of supermassive black hole seeds at high redshift to be adequately sampled in a reasonable amount of time. In a 1-deg^2 field, Lynx is predicted to detect on the order of 10^3 seeds with a mass of M ≈ 3×10^4 $M_\odot$ at $z \sim 8$ to 10. Lynx will enable a 100-fold increase in survey depth over the deepest Chandra fields, whereas ATHENA will be confusion- and background-limited before reaching the current Chandra deep field sensitivity (Fig. 4).

The large FOV and off-axis angular resolution capability for Lynx is enabled using shorter mirror segments and by changing the telescope geometry from a Wolter Type I, which Chandra uses, to a Wolter-Schwarzschild configuration. Wolter Type I configurations use a paraboloidal primary mirror coupled to a confocal hyperboloidal secondary mirror to provide excellent on-axis imaging but suffer from coma, astigmatism, and other aberrations that negatively impact off-axis performance. The Wolter-Schwarzschild configuration provides a much flatter best-focus surface because it does not suffer as much from spherical aberration and coma. This is because the Wolter-Schwarzschild design consists of two coaxial, aspheric mirror surfaces that satisfy the Abbe sine condition that states that the sine of the incident angle must be proportional to the sine of the outgoing angle.[30–32] The Lynx point spread function (PSF) for the low-energy end of the bandpass (0.2 to ∼2 keV) is expected to be better than 1 arc sec HPD to a field radius of at least 10 arc min (Fig. 5 "Lynx outer mirror" curve).
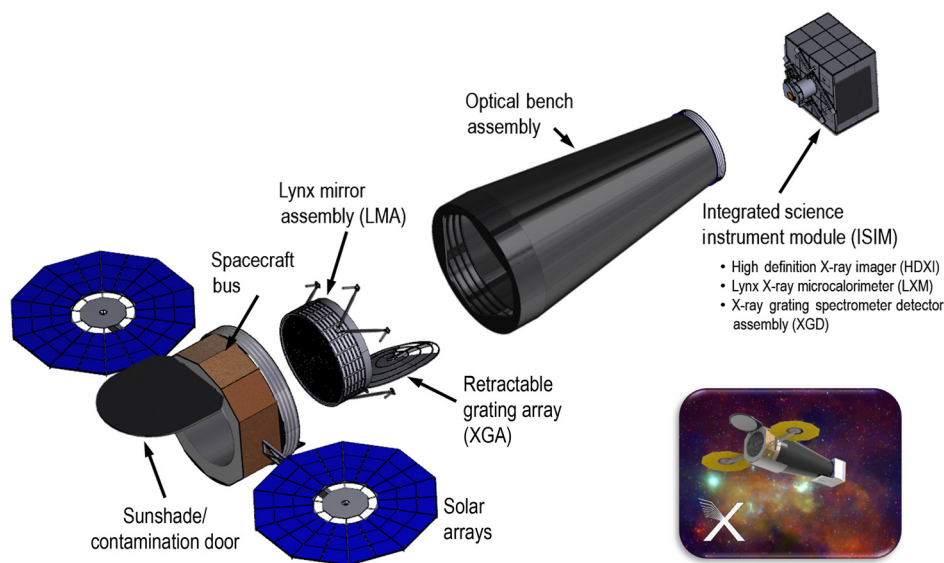

Fig. 3 Lynx x-ray observatory configuration. The LMA consists of a high-resolution, large area XMA with pre- and postcollimators, an AFT contamination door, and a retractable grating array. The LMA is surrounded by the spacecraft bus and is complemented by an instrument suite that includes HDXI, LXM, and XGS. The inset is an illustration of Lynx with all elements included (credit: NASA/M. Baysinger).
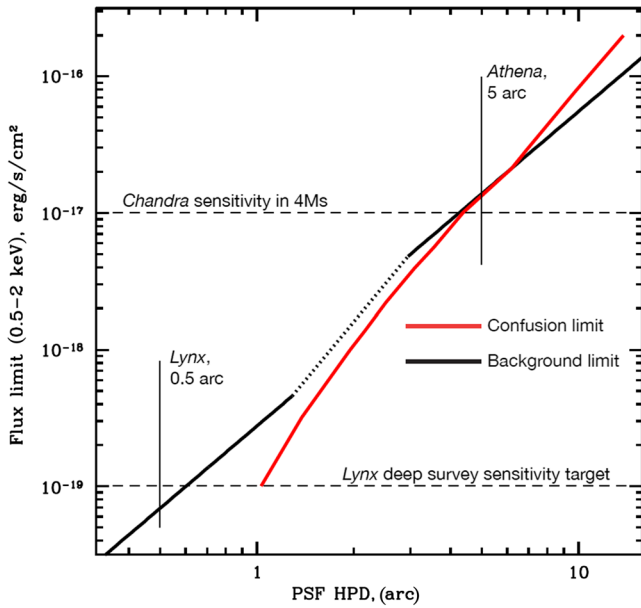
Fig. 4 The elongated pointers indicate where Lynx and ATHENA are background limited. Lynx will not be confusion limited at the required sensitivity for deep surveys of the first supermassive black hole seeds. Changes in slope for the background limit correspond to different fractions of the cosmic x-ray background resolved into discrete sources for different values of angular resolution (credit: SAO/A. Vikhlinin).
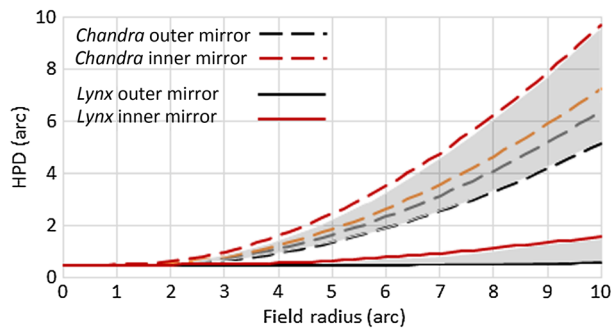

Fig. 5 Chandra Wolter Type I and Lynx Wolter–Schwarzschild angular resolution as a function of field radius are shown. The flatter Lynx response is a powerful improvement over Chandra that will permit wide-field high-redshift surveys and efficient imaging of extended sources at high-angular resolution. Chandra has four mirrors, each indicated by a dashed line. Lynx will have hundreds to tens of thousands of mirror segments, and so only the response for the inner- and outer-most mirrors is shown. The larger diameter, or outer, mirrors provide more effective area for reflecting lower energy x-rays, whereas the smaller diameter, or inner, mirrors have less effective area but are more efficient at reflecting the higher-energy x-rays (credit: Chandra mirrors—MIT/M. Schattenburg, Lynx mirrors—GSFC/W. Zhang).

Lynx's improved sensitivity will enable a large range of science observations, including the detection of sources undetectable by Chandra. An example of this has been illustrated using the Evolution and Assembly of Galaxies and their Environments (EAGLE) simulations[33] (Fig. 6). Simulated x-ray images of a 3×10^{12} M$_\odot$ elliptical galaxy at high redshift from Chandra (ACIS-I at launch) and Lynx (HDXI) indicate that the Chandra observation of this galaxy would be background dominated,

whereas the Lynx observation clearly shows the galaxy and even hints at its morphology.

The LMA is designed to preserve the sharp vision of Chandra on-axis and extend it to the entire FOV while also increasing the collecting power with significantly increased effective area. These attributes are critical to addressing the Lynx science goals outlined in Sec. 1.1, which will address fundamental questions regarding the formation and evolution of black holes, galaxies, and large-scale structure.

2.1.1 *Multiple choice x-ray mirrors*

Chandra has already achieved on-axis subarcsecond angular resolution as required by Lynx and has been operating for nearly 20 years. The Chandra full-shell mirrors were directly fabricated out of Zerodur glass, cut and polished to thicknesses ranging from 16 to 24 mm, and coated with iridium.[34] The main difference between Chandra and Lynx, other than the optical prescription, is that Lynx must achieve the same angular-resolution as Chandra but with much thinner mirrors. Thinner mirrors can be packed closer together to maximize the effective area and result in a relatively lightweight and compact assembly (Fig. 7). This, as well as being larger in diameter, is what allows Lynx to meet its effective area requirement while saving on XMA mass. This relatively lightweight, compact observatory can be launched on a standard heavy-class rocket, similar to a Delta IV Heavy, with a standard 5-m fairing, maximizing science for the cost.

Compared to mirror assemblies for Chandra,[35] XMM-Newton,[36] and ATHENA,[37] Lynx is planning to have a larger effective area at 1 keV and at least as good angular resolution on-axis as Chandra and improved angular resolution off-axis (table in Fig. 7). This combination gives Lynx its high-wide-field sensitivity. This capability combined with high-spectral resolution (Sec. 2.2) further distinguishes Lynx and will ensure that the astronomy community is provided with an observatory that will be relevant well into, and beyond, the 2030s. Lynx will be capable of addressing some of the most pertinent topics in astronomy as summarized in Sec. 1.1 and described in more detail the Lynx Final Report.[3]

There are several mirror technologies currently being developed that can meet Lynx requirements. For the purposes of this concept study, the Lynx team has focused on three technologies that have a long history of development and are currently being funded. These mirror technologies have been reported on in the previous publications, are highlighted in this special section as well, and are silicon meta-shell optics,[4] full-shell optics,[5,6] and adjustable optics.[7,8] A brief summary of each is provided below.

Silicon meta-shell optics. This technology, which is being developed by a team at GSFC, combines advanced polishing technology with monocrystalline silicon, whose near-zero internal stress enables the fabrication of extremely thin optics using modern deterministic polishing technology. Silicon also has other highly desirable properties, including a low coefficient of thermal expansion, high-elastic modulus, high-thermal conductivity, and low density. The mirror segment fabrication process, similar to the wafer manufacture process of the semiconductor industry, starts with a block of silicon measuring 150 mm × 150 mm × 75 mm. After it is ground and lapped into a conical form, it is light-weighted, etched, polished, and trimmed to the required dimensions of 100 mm × 100 mm × 0.5 mm. The trimmed mirror segment then undergoes ion beam figuring to meet figure requirements. The lightweight mirror segment is then coated with extremely low-stress coat to
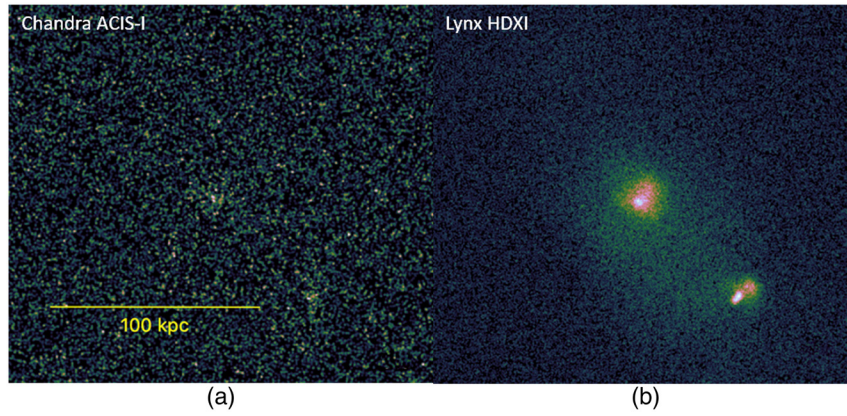
Fig. 6 EAGLE simulation of a 3×10^{12} M$_\odot$ elliptical galaxy as imaged by (a) Chandra ACIS-I and (b) Lynx HDXI. The Chandra image is background dominated, whereas Lynx can easily distinguish the galaxy (credit: SAO/J. Zuhone, CU Boulder/B. Oppenheimer).
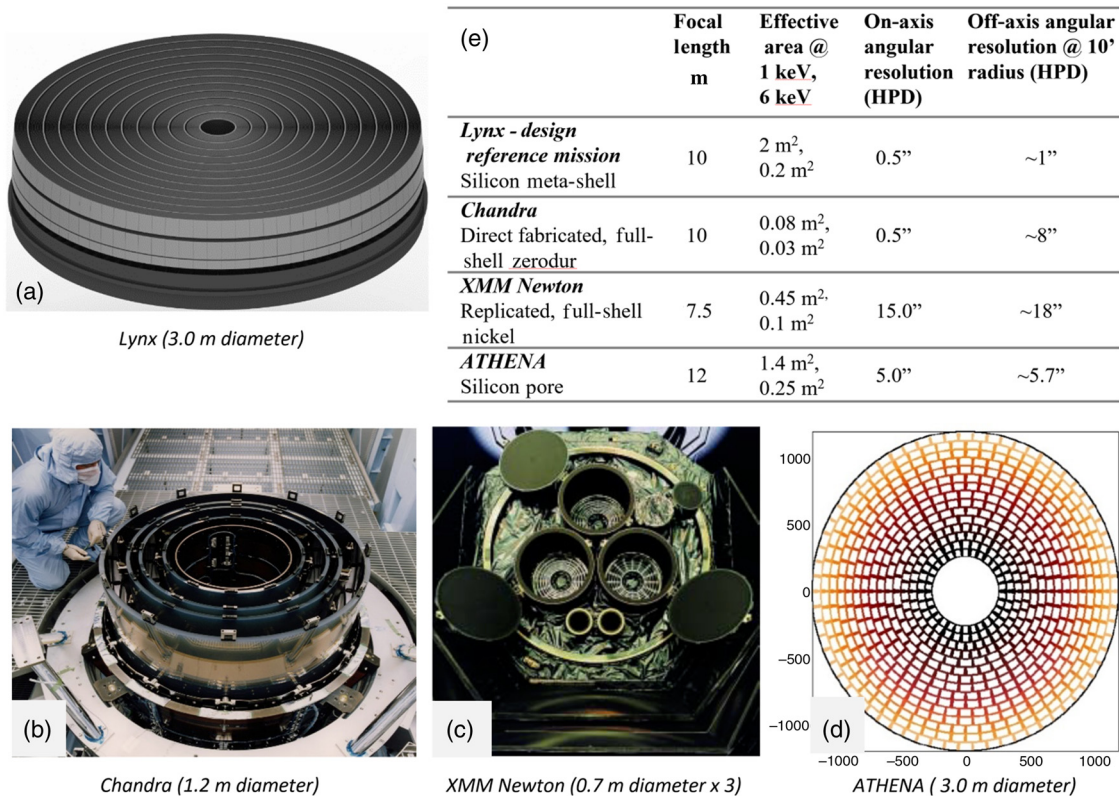

(e)	Focal length m	Effective area @ 1 keV, 6 keV	On-axis angular resolution (HPD)	Off-axis angular resolution @ 10' radius (HPD)
Lynx - design reference mission Silicon meta-shell	10	2 m², 0.2 m²	0.5"	~1"
Chandra Direct fabricated, full-shell zerodur	10	0.08 m², 0.03 m²	0.5"	~8"
XMM Newton Replicated, full-shell nickel	7.5	0.45 m², 0.1 m²	15.0"	~18"
ATHENA Silicon pore	12	1.4 m², 0.25 m²	5.0"	~5.7"

Lynx (3.0 m diameter)

Chandra (1.2 m diameter)

XMM Newton (0.7 m diameter x 3)

ATHENA (3.0 m diameter)

Fig. 7 Unlike (b) Chandra and (c) XMM-Newton that use a more traditional Wolter Type-I geometry, (a) Lynx and (d) ATHENA use a Wolter-Schwarzschild configuration that results in a significantly improved off-axis response. Fine on- and off-axis angular resolution combined with two orders of magnitude increase in effective area over that of Chandra, provides Lynx with the sensitivity needed to carry out its ambitious science case and is one of the primary features that distinguishes it from existing and planned x-ray observatories. (e) Table summarizes key parameters for Lynx, Chandra, XMM-Newton, and ATHENA x-ray observatories.

maximize x-ray reflectivity.[38,39] As of February 2019, mirror segments of surface quality comparable to or better than those of the Chandra mirrors have been made repeatedly.[4,40] Each mirror segment is kinematically supported for alignment and then permanently bonded at four locations onto a silicon plate, which serves as the structural backbone of a mirror module. The entire LMA consists of 611 such modules, and the total number of mirror segments is 37,492. This technology is highly amenable to mass production. Multiple, parallel, production lines at multiple locations will be used to optimize mirror segment

Full-shell optics. Currently being developed by INAF/Brera and MSFC, full-shell optics are geometrically most similar to those of Chandra. Just as the name implies, full-shell optics are not made up of individual mirror segments but are full cylindrical-like revolutions. The primary advantages are that there are

many fewer mirrors (a couple hundred) to fabricate and mount, and due to their geometry, these optics are intrinsically less sensitive to coating stress and mounting-induced distortion relative to the mirror segment approach. There are multiple full-shell technologies that have the potential to meet Lynx requirements, two of these are direct fabrication and replicated. Relatively thick (16 to 24 mm) direct fabricated full-shell optics that yield subarcsecond angular resolution have been demonstrated on Chandra. The primary challenge for Lynx is to maintain this performance on thinner, larger diameter mirrors. One technique for the direct fabrication of x-ray optics requires annealing a cylindrical fused silica or ultralow expansion glass and etching it to the correct figure. This is followed by fine grinding, polishing, ion beam figuring, and coating. The best result to date on a thin (2 to 3 mm) fused-silica full-shell mirror is ~18 arc sec HPD, measured using x-rays. This measurement was made prior to final polishing due to the mirror shell being damaged during testing.[5] Replicated full-shell optics are made by an entirely different process and have a different set of benefits and challenges.[6,41,42] The best performance to date is individual replicated mirror shells that have around 8 arc sec HPD and larger (>1 m) diameter replicated optics have yet to be proven.[6] Surface treatments such as differential deposition and ion milling can further improve performance.[43,44]

Adjustable optics. This class of x-ray optic allows for *in situ* adjustability of thin segmented[7] or full-shell[45] optics. For this study, the Lynx team focused on adjustable segmented optics being developed at the SAO. These optics are made by coating a thin, 0.4-mm, curved glass substrate with an x-ray reflective coating on the front side and a film of piezoelectric actuators (lead-zirconate-titanate—PZT) in an array pattern on the back. The application of the front reflective coating helps to offset the stress induced by the piezoelectric film coating. Voltage modulators can be deposited on top of the piezoelectric film to allow for control of the actuation. The main advantage of this type of optic is that the adjustability can be used to correct for certain mirror figure errors in the optic introduced during the fabrication process and to reduce mounting-induced distortions, making it easier to achieve subarcsecond performance. The ability to adjust can also potentially lead to shorter production and installation times, saving on cost and schedule. The development of these optics at SAO has yielded proof-of-concept results that demonstrate the ability to predict and control a thin mirror segment to a very high precision.[46,47] The simulated image

quality based on this demonstration approaches that required by Lynx.[48] The team at SAO is working on improving the mounting process and the production process and deposition of the PZT that currently distorts the mirror figure just outside of the range of correctability. Key challenges include assembly of the 12,720 mirror segments and demonstration through x-ray imaging of a fully mounted, adjustable mirror pair.

All of these mirror technologies are currently at a TRL > 2 and all are expected to meet or exceed TRL 3 or TRL 4 by the early 2020s.

2.1.2 *X-ray mirror trade study*

The selection of a single mirror technology for the Lynx DRM was necessary to focus the concept and to provide at least one end-to-end architecture that could be costed and integrated into the program schedule. Deciding which mirror technology to use for integration into the DRM required careful scrutiny, as each technology that the team studied has unique advantages, challenges, and different development paths for maturation. The Lynx team opted to use the Kepner-Tregoe[49] decision-making strategy for this trade study. This strategy uses a systematic approach to reaching group consensus on key differentiating criteria to satisfy a decision statement formulated by the stakeholders. The stakeholders for this study were members of the Lynx STDT, and the decision statement, or goal, was for the trade study team to recommend one DRM concept mirror architecture to focus the design for the Lynx final report and to identify all feasible alternates.

Trade study criteria included science, technical, and programmatic requirements. Each of these was broken down into two categories: absolute "musts" and relative "wants." The musts, of which there were 8 criteria (Table 1), were required to be met and are pass/fail. The wants, of which there were 18 criteria (not shown here), had relative weightings and offered a comparative assessment between the technologies, including an estimated cost for the development. Risks and opportunities were identified during this process and were an integral part of the evaluation.

Each of the Kepner-Tregoe criteria was evaluated by a large team of experts chartered by the Lynx STDT. The evaluation team was a mixture of individuals both external and internal to the Lynx Program. They were volunteers from industry, the Lynx STDT, Universities, and NASA Centers. Many of

Table 1 Lynx mirror technology trade criteria Kepner-Tregoe musts. Each of these musts had to be met and demonstrated to the Lynx Mirror Architecture Trade Team, or else be eliminated as a feasible technology for Lynx.

Science	Optical performance meets the requirements flowing down from Science traceability matrix
Technical	Credible roadmap from present status to the achievement of on-orbit requirements
	Performance modeling tools related to current results are demonstrated to be credible
	Repeatable fabrication process based on current status
	Credible error budget that flows down to each mirror element
	Expected to survive launch
Programmatic	Credible plan to meet TRL 4-6
	Produce the mirror assembly within the program schedule allocation

these individuals were instrumental in the formulation and construction of Chandra and have worked on other large flight programs. The process was facilitated by G. Blackwood at JPL, who had no affiliation with the technologies under consideration. The study was carried out over 6 months and took roughly 5000 person-hours to complete. Over the course of the study, more than 650 pages of material were produced by the development teams.

The trade study recommended the silicon meta-shell optics for the DRM. The Full-Shell Optics and Adjustable Optics concepts were both deemed feasible alternates. This decision was reviewed by the STDT and accepted by the STDT Chairs. Selection of a mirror technology for the DRM does not indicate which technology should or will be used for flight. That decision will only be made after selection of the Lynx mission, in which point each of these technologies, as well as others outside of this study, would be assessed and competed.

2.2 Science Instruments

Complementing the LMA is the suite of highly capable science instruments. This suite of instruments includes the large-scale active sensor pixel array—HDXI, the high-spectral resolution grating spectrometer—XGS, and the imaging spectrometer—LXM. For maximum flexibility in operation, HDXI and LXM can be translated into and out of the focal plane as needed. A focus mechanism attached to this table allows for fine focus adjustment of these instruments. The XGS grating array can be actuated into and out of the optical path, and its detector assembly, which is mounted to a fixed portion of the ISIM, has an independent focus adjustment. All of these instruments are currently being funded for development and have a plan for maturation that is consistent with the overall schedule and cost for the Lynx observatory.[25] Even though these instruments all require some degree of development to meet Lynx requirements, each is a natural evolution of existing or planned flight instruments.

2.2.1 High-definition x-ray imager

Silicon-based x-ray imaging spectrometers are standard for nearly every x-ray observatory that has flown or is currently flying. Some examples include Chandra's advanced CCD imaging spectrometer-ACIS,[50] XMM-Newton's EPIC MOS[51] and pn[52] Cameras, and Suzaku's x-ray imaging spectrometer-XIS.[53]

All of these instruments use traditional x-ray CCDs, which have good spectroscopic performance and imaging capability but have relatively low-readout rates. For x-ray observations in the energy range probed by Lynx and ATHENA, APS offer high-readout rates, low-noise, high-broadband quantum efficiency, and minimal cross talk compared to traditional CCDs.

ATHENA's wide field imager (WFI) will use depleted field effect transistors (DEPFETs) that are more than capable of meeting ATHENA's superb FOV and imaging resolution requirements.[54] However, the Lynx HDXI requires a detector that can accommodate smaller pixels that can appropriately oversample the telescope's PSF. The natural choice, based on the current state-of-the-art and maturation path, is to use an array of monolithic or hybrid pixelated CMOS-based active sensors or digital CCDs with CMOS readout. HDXI detector candidate technologies are described in detail in this paper and elsewhere in the literature.[9–12] These detectors will be able to provide a low-noise, wide FOV, high-count rate capability (8000 ct s^{-1}) option and will be able to support the high-angular resolution required by Lynx with ~0.3 arc sec pixels. Key requirements for Lynx and ATHENA APS arrays compared to Chandra's ACIS-I array are summarized in Table 2.

Both x-ray CCDs and APS can be arrayed to accommodate each observatory's FOV requirement, as it is illustrated in Fig. 8. The baseline configuration for HDXI is an array of 21 APSs, needed to meet the Lynx FOV requirement. These sensors are tiled to follow the curved focal surface, maximizing the angular resolution response across the FOV. However, this is not the only possible configuration for HDXI. Rather, it may be possible to use fewer, larger sensors, for potentially lower cost, the implications of which are being explored. A design consideration that the Lynx team considered is a larger FOV. The HDXI FOV can be increased but at a cost to the program. Balancing the observatory capabilities with cost is critical and is in-line with the Lynx team's design philosophy to maximize the science for a reasonable and affordable cost to the community.

High-angular resolution across the Lynx FOV, enabled by the mirrors and HDXI, allows for larger, deeper surveys needed to directly detect the seeds of supermassive black holes (Fig. 9). HDXI must have a large FOV (22×22 arc min) and pixel-size that adequately oversamples the PSF.

The moderate spectral resolution of HDXI across the Lynx 0.2- to 10-keV band will allow the thermodynamic properties of

Table 2 Lynx's HDXI will use APS technology based on CMOS or digital CCD + CMOS readout. These detectors are able to meet the Lynx requirements for high-resolution imaging while maintaining good energy resolution, low-noise, and good time resolution. Although ATHENA's WFI will also use APS technology, it uses DEPFETs, which are not yet sufficient to meet Lynx's PSF requirements. Chandra's ACIS-I uses a traditional x-ray CCD, which is sufficient to meet the resolution requirements but has much poorer time resolution.

	FOV (arc min)	Pixel size (μm)	Energy resolution (FWHM)	Read noise	Time resolution
Lynx-HDXI	22×22	16×16	~70 eV at 0.3 keV,	$\leq 4e^-$	20 ms (full-field)
			150 eV at 5.9 keV		200 μs (window mode)
Chandra-ACIS-I	16.9×16.9	24×24	130 eV at 1.49 keV	$<2e^-$	3.2 s (full frame ACIS I)
			280 eV at 5.9 keV		
ATHENA-WFI	40×40	130×130	≤ 80 eV at 1.0 keV	$2.5 e^-$	<5 ms (large detector)
			170 eV at 7.0 keV		80 μs (high-count rate sensor)

Lynx - HDXI

(a)

Chandra - ACIS

(b)
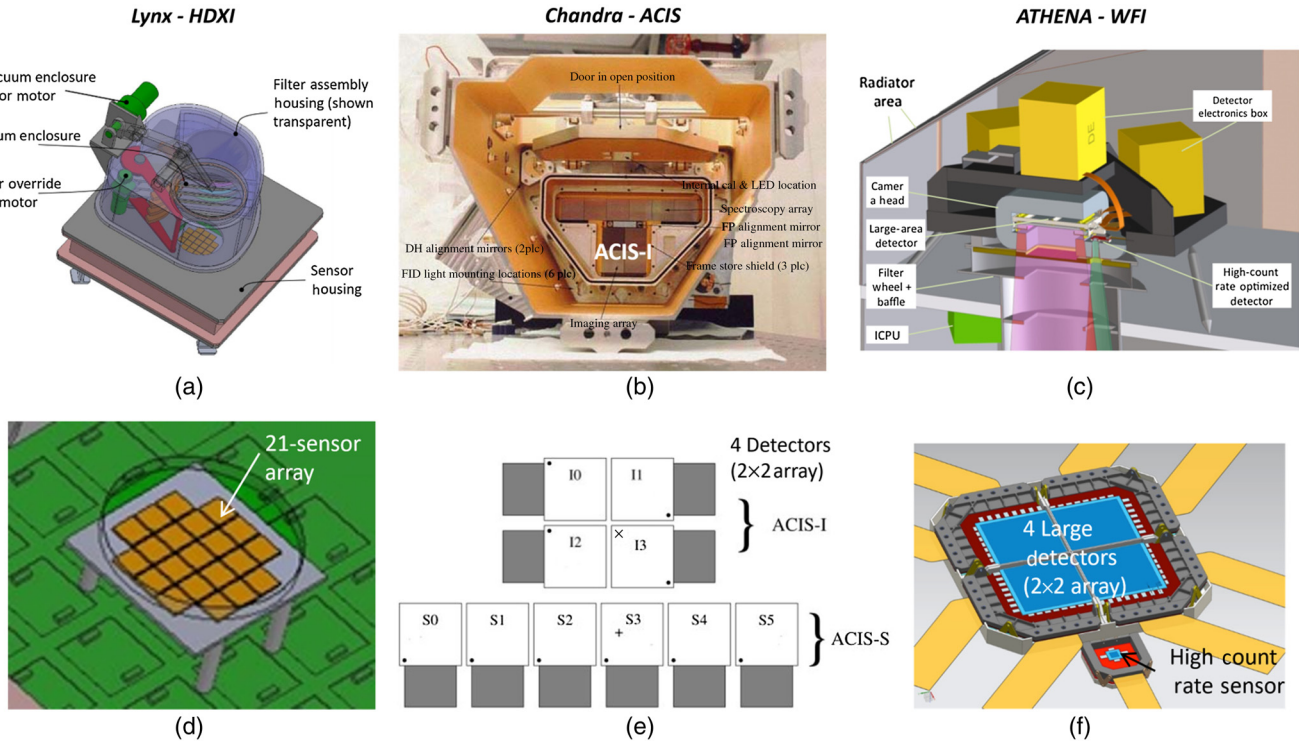
ATHENA - WFI

(c)

(d)

(e)

(f)

Fig. 8 Mechanical layouts for (a) and (d) Lynx compared to (b) and (e) Chandra's ACIS and (c) and (f) ATHENA's WFI and illustrates the similarities in how detectors are tiled to meet FOV requirements for each observatory. The baseline for HDXI uses 21 CMOS-based sensors tiled in an array, which allows the detectors to be tiled to match the curvature of the focal surface (credit: Lynx HDXI—NASA/Chandra ACIS—NASA/ATHENA WFI—ESA).
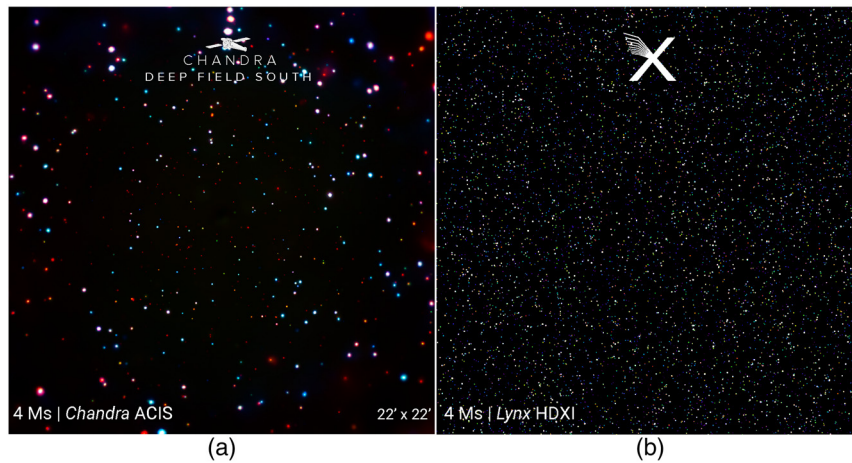

(a)

(b)

Fig. 9 (a) Chandra deep field—South, 4 Ms image clipped at the HDXI FOV of 22×22 arc min. This image clearly shows a broadening in the PSF beyond the central ~2.5 arc min region, which is due to the Wolter Type-I geometry of the Chandra high-resolution mirror assembly. (b) A simulated 4 Ms Lynx HDXI image that illustrates a flatter response across the FOV, and the detection of many more, and higher z sources due to the increased sensitivity (credit: SAO/Trembley/Vikhlinin/Zuhone).

the hot gas in galactic halos and other extended objects to be characterized, whereas the high time resolution will allow for the observation of bright x-ray binaries and compact sources with minimal pile-up.

2.2.2 X-ray grating spectrometer

Over the past 20 years, both of Chandra's transmission grating spectrometers [using the low-energy transmission gratings (LETG) and the high-energy transmission gratings (HETG), where the later consists of two assemblies: the high-energy grating (HEG), and medium energy grating (MEG)] and XMM-Newton's reflection grating spectrometer (RGS) have provided the astronomy community with high-resolution x-ray spectroscopy resulting in countless discoveries.[23,55–57] In order to access discovery space beyond Chandra and XMM-Newton, future observatories must be designed to be even more capable. The
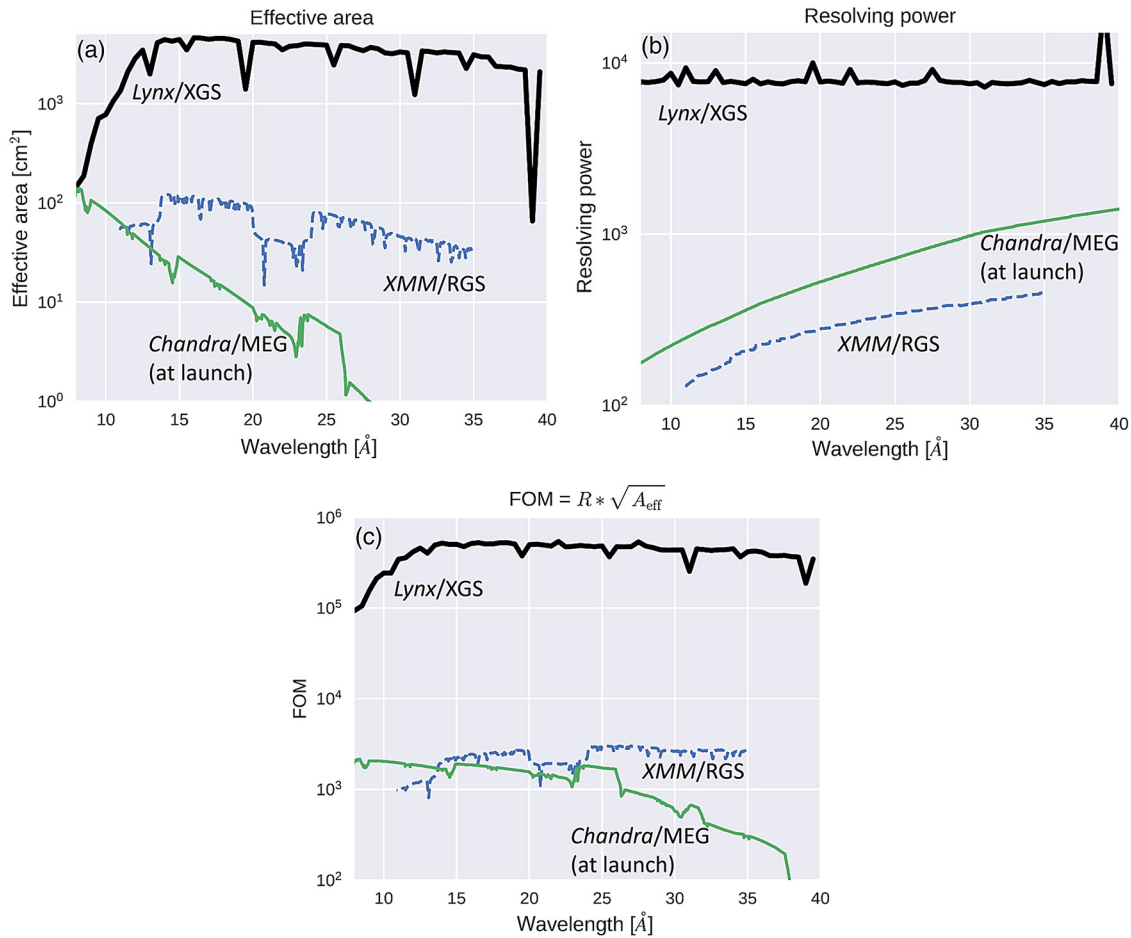
Fig. 10 The effective area (a) resolving power (b) and the line detection figure of merit (c) predicted for a Lynx XGS built using the CAT gratings for the DRM. These plots show large increases in capabilities that Lynx would have over those obtained with the Chandra and XMM-Newton grating instruments (credit: MIT/H. M. Günther).

Lynx XGS will exhibit significantly enhanced resolving power ($R \geq 5000$) and a much larger effective area (≥ 4000 cm^2 at 0.6 keV) (Fig. 10). Lynx XGS will characterize the warm gas in galactic halos out beyond their virial radius through absorption line studies of background AGNs, which requires high spectral resolution and sensitivity in the 0.2- to 2.0-keV band, capable of 1-mÅ sensitivity in key absorption lines of OVII and OVIII. XGS will be able to carry out transformational science that includes these studies on the warm hot intergalactic medium and will expand our knowledge on active star forming regions, stellar coronae, and the impact of x-ray and extreme ultraviolet flux and winds on planet habitability.[2,3]

These increases in performance are made possible through recent developments in reflection[13] and transmission[14] grating technologies, both of which are able to meet Lynx's requirements. Critical angle transmission (CAT) gratings being developed at MIT have been baselined for the Lynx DRM for purposes of program costing and scheduling. Reflection gratings that operate in an off-plane geometry (OP) being developed at PSU offer equally high performance. Much like the Lynx mirrors, the XGS technology will be competed once Lynx has been selected for funding.

Similar to Chandra's design, the Lynx gratings are affixed to a single retractable door (Fig. 11). Effort has been made to keep the mechanism simple for this door while maintaining precise positioning each time the gratings are deployed. The actuator used to deploy the gratings array door allows for 1.2-μm-level positioning for high repeatability. A second actuator has been added for redundancy. Lynx CAT and OP gratings have an alignment tolerance of roughly 100 to 200 μm along the optical axis, well within the capability of these actuators.

The Lynx XGS will have a dedicated detector array located on a fixed platform on the ISIM. An optical blocking filter will be used to block stray light from getting into the detector, which can adversely affect the resolving power. The detector array will also have an independent focus adjustment mechanism with a range of ± 0.4 in. The detector technology will leverage that of HDXI to save on cost. The detector geometry is discussed in detail in the previous papers and in the Lynx final report.

Chandra's HETG/LETG and XMM-Newton's RGS are shining examples of x-ray missions that have successfully flown and operated large-scale grating spectrometers (Fig. 12). These instruments demonstrate that scaling individual gratings to large arrays is not an insurmountable challenge. Scaling to the large areas required by the Lynx XGS is addressed by both technologies in their respective technology roadmaps. The same manufacturing algorithm that will be applied to the Lynx mirror segments (see Sec. 1.4) can be applied also to the XGS gratings to optimize cost and schedule, and to reduce risk.
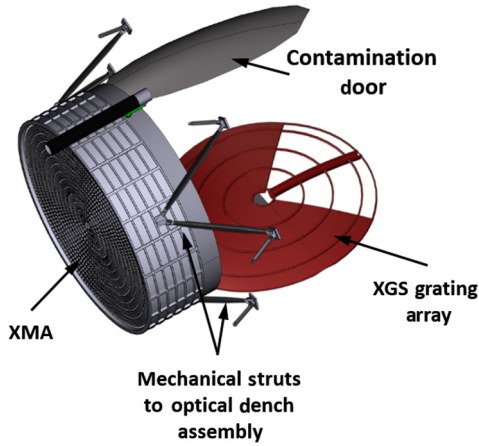
Fig. 11 Conceptual drawing of the LMA with the XGS grating array shown. The gratings can be retracted when not in use (credit: NASA MSFC/M. Baysinger/J. Rowe).

2.2.3 *Lynx x-ray microcalorimeter*

In addition to high-angular resolution, large FOV imager and large area, high-energy resolution dispersive spectrometer, Lynx will showcase a nondispersive imaging spectrometer or x-ray microcalorimeter. The true power of the x-ray microcalorimeter was first realized by the soft x-ray spectrometer (SXS) on the JAXA Hitomi (Astro-H) mission, when it revealed the high-resolution (4.9-eV FWHM at 6 keV) spectrum of the core of the Perseus cluster, tightly constraining the velocity dispersion of the cluster gas.[58] Building on the successful

implementation of Hitomi's SXS, the ESA planned ATHENA observatory is including an x-ray microcalorimeter, x-ray integral field unit (X-IFU), in their payload that is well-matched to ATHENA's large FOV and higher angular resolution. X-IFU is a different design than that of the SXS, as it has many more pixel elements to read out and requires an even higher energy resolution.[59–61] The LXM is the most capable yet, as the Lynx science case requires LXM to have an FOV comparable to the X-IFU (Fig. 13) but matched to the order-of-magnitude higher angular resolution exhibited by the Lynx telescope. LXM must also provide an even higher energy resolution, necessary to address some of the most compelling and unanswered science questions regarding fundamental drivers of galaxy and large-scale structure formation and evolution. However, a finer angular resolution combined with a relatively large FOV translates into an increased number of pixel elements over that of the X-IFU (Table 3). Fortunately, due to innovative thermal multiplexing using hydras, the number of pixel readouts for LXM is reduced to just 2× that of the X-IFU.[15]

The LXM must be able to spatially resolve AGN feedback signatures from surrounding hot gas and jets in galaxies, groups, and clusters on 1 arc sec or finer scales, resolve starburst-driven winds in low-redshift galaxies at a high-spectral resolution of ~0.3 eV over ~1-arc min FOVs (at 1-arc sec imaging resolution), map metallicity gradients (better than 5-eV resolution over 5-arc min FOV) in circumgalactic, group, and galaxy cluster fields, and survey young SNRs in local group galaxies.

LXM has baselined an architecture with three sensor arrays that meet the combinations of spectral, spatial, and FOV required by these transformational science goals. The "main
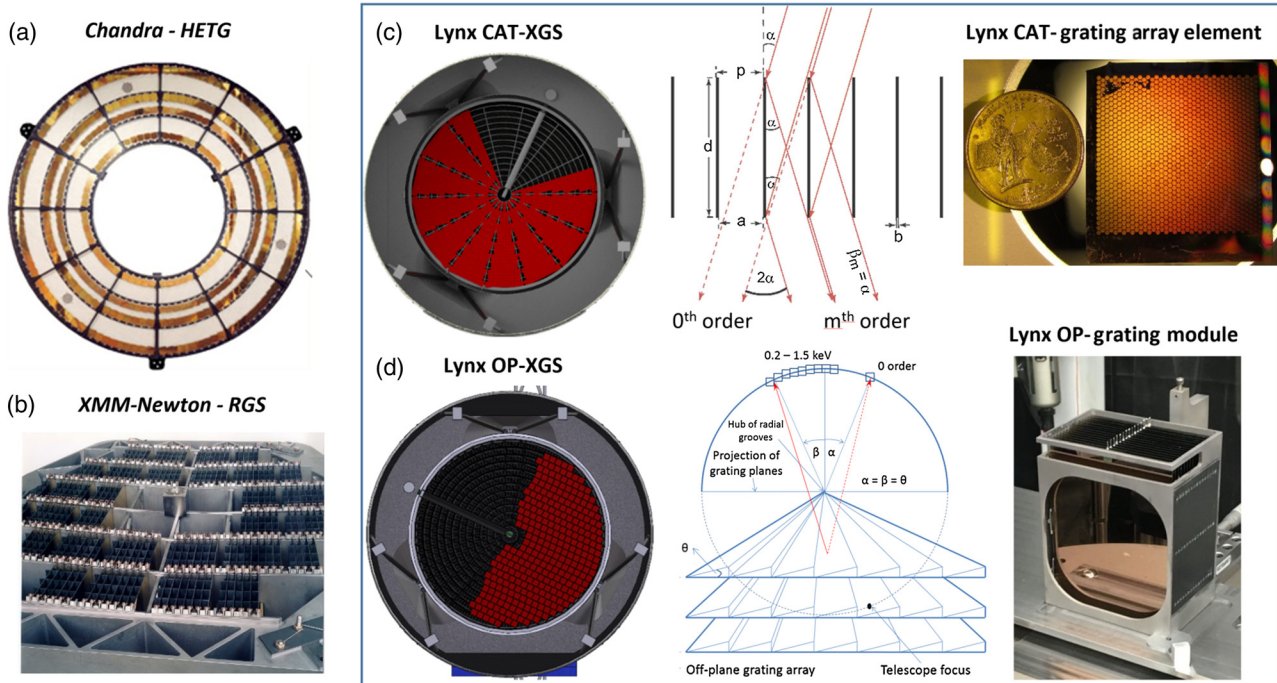

Fig. 12 (a) Images of Chandra's HETG and (b) XMM-Newton's RGS. These large-scale structures have been successfully operating for over 20 years on orbit. Like these instruments, Lynx will use either transmission (c) or reflection (d) gratings, but using different technologies, and will require a much larger grating effective area. Depending on the technology selected for Lynx, different mirror coverages may be required. The current design requires ~73% mirror coverage of the CAT gratings (baseline for the DRM), and ~50% coverage for the OP gratings (credit: Chandra HETG/NASA, XMM-Newton RGS/ESA, Lynx CAT- and OP-XGS drawings/NASA, Lynx CAT-XGS image/MIT, and OP-XGS image/PSU).
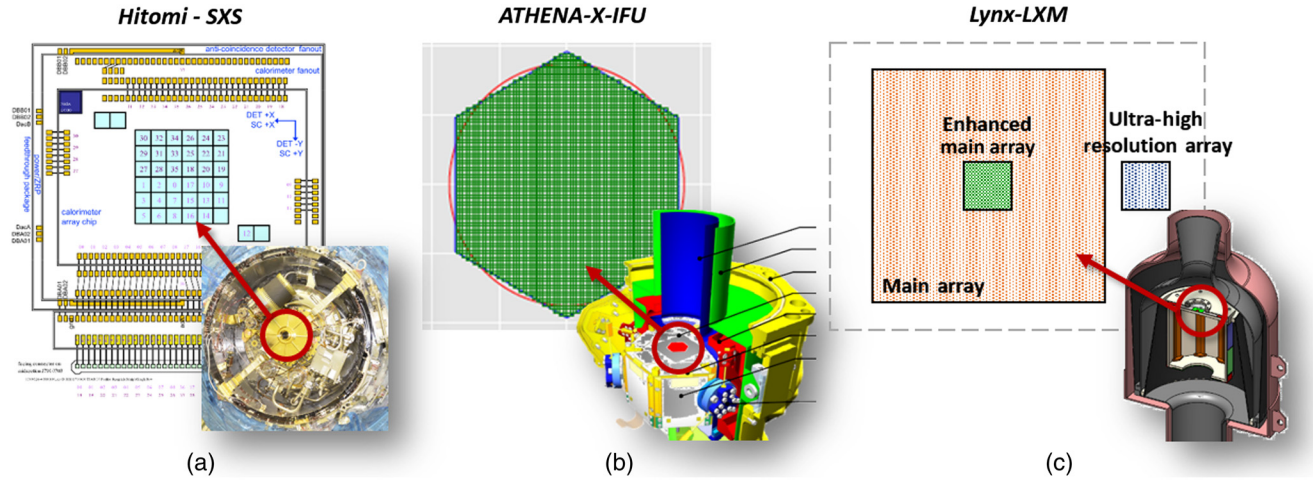
Fig. 13 Sensor geometries for (a) Hitomi's SXS, (b) ATHENA's X-IFU, and (c) LXMs are shown. The Lynx baseline configuration has three arrays that are designed to complement the telescope's FOV and high-angular resolution while exhibiting high-energy resolution. The LXM "main array" will match the X-IFU's FOV and will have roughly the same number of readout channels. The number of readout channels for the LXM "enhanced main array" combined with that of the "ultrahigh-resolution array" doubles the number of readout channels required for this instrument (credit: Hitomi-SXS/JAXA, ATHENA-X-IFU/ESA, and Lynx-LXM/NASA).

Table 3 LXM will have three sensor arrays that share the focal plane. These arrays exhibit a combination of FOV, angular resolution, and energy resolution as required to meet the Lynx science goals. For comparison, characteristic parameters for ATHENA's X-IFU and Hitomi's SXS are included.

		FOV (arc min)	# of readout channels (# pixel elements)	Pixel size (effective angular resolution)	Energy resolution (FWHM)
Lynx—LXM	Main array	5	3456 (86,400)	50 μm (1 arc sec)	3 eV (0.2 to 7 keV)
	Enhanced main array	1	512 (12,800)	25 μm (0.5 arc sec)	~2 eV (0.2 to 7 keV)
	Ultrahigh-resolution array	1	3600 (3600)	50 μm (1 arc sec)	0.3 eV (0.2 to 0.75 keV)
ATHENA—X-IFU		~5	3840 (3840)	245 μm (~5 arc sec)	2.5 eV at <7 keV
Hitomi (Astro-H)—SXS		3	36 (36)	814 μm (~1.2 arc min)	<7 eV at 6 keV

array" will provide a large FOV with good angular resolution and energy resolution across the Lynx bandpass. The "enhanced main array" has a narrower FOV but an angular resolution that is precisely matched to that of the Lynx telescope. The "ultrahigh-resolution array" has the same reduced FOV as the "enhanced main array" but with much higher energy resolution at lower energies (Table 3).

LXM will take advantage of developments from both Hitomi's SXS and ATHENA's X-IFU. One example of this is the modulated x-ray source (MXS) that will be included on the LXM focal plane assembly for in-flight calibration by providing pulsed x-ray lines at multiple energies. The MXS will be similar to that used on Hitomi's SXS[62,63] and on the planned ATHENA mission.[61] Another design element that LXM can leverage is the X-IFU readout layout (similar wire density and flex cable technologies), due to the similar focal plane sizes. Similar focal plane size also allows for the mechanical, thermal, magnetic shielding, anticoincidence detector, and IR filter designs to be leveraged. The requirement that the LXM needs to be cooled to 50 mK can be met with a cryostat that uses heritage from the Hitomi SXS and design details from the ATHENA X-IFU. Like

the SXS and the X-IFU, LXM will also need to be cooled to a temperature of 50 mK, allowing the instrument to use a cryostat that takes advantage of Hitomi heritage. Other elements of the cooling system will be achieved via a thrust-tube type design mounted in a fashion similar to that used for Spitzer. All LXM elements are detailed in multiple papers of this section, as is a comprehensive overview of this ambitious, yet highly feasible instrument.[14–20]

3 Lynx Mission

3.1 Journey to Sun–Earth L2

Based on a preliminary program schedule, Lynx is planning to launch in the mid-2030s and the current assumption (still under evaluation) is that Lynx will be integrated onto a heavy class (expendable or recoverable) vehicle that will launch from NASA Kennedy Space Center. Following a transfer trajectory insertion maneuver, Lynx will be inserted into the 800,000-km semimajor axis halo orbit around the SE-L2 libration point and will operate for 5 years with consumables for 20 years.
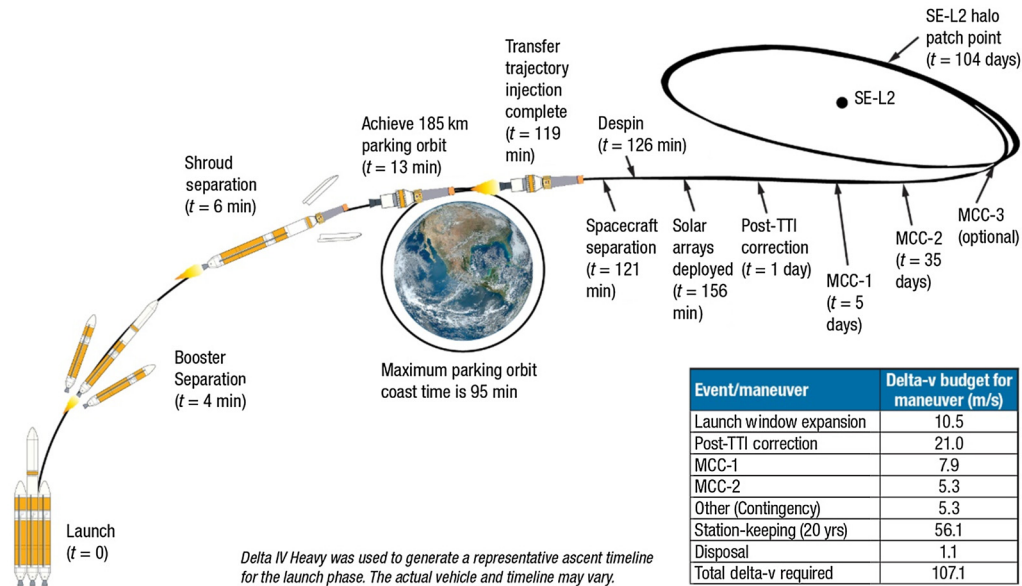
Fig. 14 Launch to orbit timeline and delta-v budget.

The launch to orbit timeline and delta-v budget is shown in Fig. 14.

Several orbits were analyzed for Lynx, including SE-L2, drift-away, lunar distant retrograde orbit, Chandra-type orbit, and transiting exoplanet survey satellite like. After careful consideration, SE-L2 was selected because it provides: (1) essentially no eclipsing, (2) a stable thermal environment, (3) avoidance of trapped radiation belts, (4) fewer maneuvers for orbit insertion and thus, relatively smaller propulsion system, and (5) a high observing efficiency of better than 85%. The observing efficiency is the percentage of actual time Lynx will spend on science observations and takes into account the estimated times for slewing, thermal and vibrational stabilization, calibration, and other applicable operational procedures.

3.2 Launch Vehicle

This timeline assumes launch on a Delta IV Heavy vehicle. Even though the Delta IV Heavy is not expected to be available in the 2030s, it is assumed to be representative of expected capability (though not necessarily cost) of the generic heavy class vehicles in the 2030s. Given the mass and volume of the Lynx observatory, it is expected that multiple suitable heavy-class vehicles, as well as the ultraheavy space launch system, will be available for use. The flexibility of Lynx to fly on multiple platforms reduces the risk of not having a vehicle to launch on in the 2030s and allows for schedule and cost to be optimized. As some of these launch vehicles have shorter payload envelopes than others, the Lynx team is performing a trade study to determine the cost and risk associated with utilizing an extendable optical bench.

3.3 Science Operations

Following on-orbit activation and checkout, Lynx will operate primarily in a nearly autonomous, preplanned science program. A typical scientific observing timeline includes a series of maneuvers between targets, target acquisition, and data collection. In this mode, the focal plane science instruments are in either a data collection or standby configuration, under control of the onboard computer. Normal spacecraft operations such as switching focal plane instruments between HDXI and LXM, instrument calibrations, momentum unloading, ground contacts, and recorder data playback all take place in normal mode.

The majority of science operations are preplanned using a scheduling process that seeks to maximize the time on-target while accommodating all necessary spacecraft operations. The mission schedule plan will be used to generate spacecraft and instrument commands, which are then uplinked to the spacecraft and stored. A sufficient number of commands will be loaded to assure autonomous operation for 72 h. Stored command loads can be interrupted and updated as needed to accommodate target of opportunity (ToO) requests (and emergencies). It is anticipated that ToO requests may require up to 24 h to initiate and review new command sequences, depending on spacecraft (thermal, power, momentum, and pointing) constraints, minimization of maneuver error, and the frequency of ground contact.

4 Integrated Approach

An integrated analysis of the Lynx architecture has been initiated via an industry CAN partnership that involves Northrop Grumman, Ball Aerospace, and Harris Corp. participation. This study enables refinements to the current design by considering the integrated observatory system and producing an error budget for the on-orbit payload performance. Integrated studies include assessing the alignment of the LMA to the focal plane, alignment of the grating arrays to the focal plane, potential thermal and mechanical instabilities on the optical bench and impact on interface design, thermal gradients on the mirror assembly, aspect system design and accommodation, and exported disturbances based on dynamic models on-orbit. This error budget will be used to update the observatory design, until all payload performance requirements are met. During this process, trades will be identified to optimize performance, cost, and schedule for the fully integrated system.

5 Summary

The Lynx architecture was chosen to meet an ambitious, yet realizable, science case to observe the first black hole seeds

in the Universe, trace the state of matter in cosmic structures, and to characterize the formation and evolution of stars and their local environments, including their planetary systems. The Lynx design is streamlined, employing relatively mature technologies for a concept phase and baselines standard spacecraft elements and heavy-class launch vehicles. The approach to design is integrative and system oriented and focused on achieving the required on-orbit performance. Further, this approach will apply the appropriate lessons learned from previous and planned missions to lower risk. Building on to the legacy of successful x-ray missions (e.g., Chandra and XMM-Newton), Lynx will carry out transformational science in the 2030s and beyond for a cost that is compatible with a balanced Astrophysics portfolio.

References

1. C. Kouveliotou et al., "Enduring quests-daring visions (NASA astrophysics in the next three decades)," arXiv:1401.3741 (2014).
2. F. Zel and A. Vikhlinin, Lynx Team, "2018 Interim Report," 2018, https://wwwastro.msfc.nasa.gov/lynx/docs/LynxInterimReport.pdf.
3. F. Zel and A. Vikhlinin, Lynx Team, "2019 Final Report," 2019, https://wwwastro.msfc.nasa.gov/lynx/.
4. W. W. Zhang et al., "High-resolution, lightweight, and low-cost x-ray optics for the Lynx observatory," *J. Astron. Telesc. Instrum. Syst.* **5**(2), 021012 (2019).
5. M. Civitani et al., "Lynx optics based on full monolithic shells: design and development," *Proc. SPIE* **10699**, 106990N (2018).
6. K. Kilaru et al., "Full-shell x-ray optics development at NASA MSFC," *J. Astron. Telesc. Instrum. Syst.* **5**(2), 021010 (2019).
7. P. B. Reid et al., "Development of adjustable x-ray optics for the Lynx mission concept," *Proc. SPIE* **10699**, 106990Q (2018).
8. N. Bishop et al., "Thickness distribution of sputtered films on curved substrates for adjustable x-ray optics," *J. Astron. Telesc. Instrum. Syst.* **5**(2), 021005 (2019).
9. A. D. Falcone et al., "Overview of the high definition x-ray imager (HDXI) instrument on the Lynx x-ray surveyor," *J. Astron. Telesc. Instrum. Syst.* **5**(2), 021019 (2019).
10. S. Hull et al., "Hybrid CMOS detectors for the Lynx x-ray surveyor high definition x-ray imager," *J. Astron. Telesc. Instrum. Syst.* **5**(2), 021018 (2019).
11. M. W. Bautz et al., "Toward fast, low-noise CCDs for Lynx," *J. Astron. Telesc. Instrum. Syst.* **5**(2), 021015 (2019).
12. A. Kenter et al., "Advancing the technology of monolithic CMOS detectors for use as x-ray imaging spectrometers," *Proc. SPIE* **10397**, 1039703 (2017).
13. R. McEntaffer, "Reflection grating concept for the Lynx x-ray grating spectrograph," *J. Astron. Telesc. Instrum. Syst.* **5**(2), 021002 (2019).
14. H. M. Günther and R. K. Heilmann, "Lynx soft x-ray critical-angle transmission grating spectrometer," *J. Astron. Telesc. Instrum. Syst.* **5**(2), 021003 (2019).
15. S. R. Bandler et al., "Lynx x-ray microcalorimeter—LXM," *J. Astron. Telesc. Instrum. Syst.* **5**(2), 021017 (2019).
16. K. Sakai et al., "Development of space-flight compatible room-temperature electronics for the Lynx x-ray microcalorimeter," *J. Astron. Telesc. Instrum. Syst.* **5**(2), 021013 (2019).
17. S. J. Smith et al., "Multi-absorber transition-edge sensors for x-ray astronomy," *J. Astron. Telesc. Instrum. Syst.* **5**(2), 021008 (2019).
18. D. A. Bennett et al., "Microwave SQUID multiplexing for the Lynx x-ray microcalorimeter," *J. Astron. Telesc. Instrum. Syst.* **5**(2), 021007 (2019).
19. T. R. Stevenson et al., "Magnetic calorimeter option for the Lynx x-ray microcalorimeter," *J. Astron. Telesc. Instrum. Syst.* **5**(2), 021009 (2019).
20. M. E. Eckart et al., "Design of optical/IR blocking filters for the Lynx x-ray microcalorimeter," *J. Astron. Telesc. Instrum. Syst.* **5**(2), 021020 (2019).
21. M. J. DiPirro, "Lynx X-ray microcalorimeter cryogenic system," *J. Astron. Telesc. Instrum. Syst.* **5**(2), 021006 (2019).
22. M. C. Weisskopf, "The Chandra x-ray optics," *Opt. Eng.* **51**(1), 011013 (2011).
23. Chandra X-ray Center, "Chandra X-Ray Observatory," http://chandra.harvard.edu/ (20 September 2018).
24. Senate and House of Representatives of the United States of America in Congress Assembled—Commerce, Science, and Transportation Committee National Aeronautics and Space Administration Authorization Act of 2010, Public Law 111-267-October 11 2010, 124 Stat. 2833, Sec. 804. In-Space Servicing, Became Public Law October 11 2010, https://www.congress.gov/bill/111th-congress/senate-bill/3729.
25. Lynx Team, "Lynx Technology Roadmaps," 2019 (in preparation) https://wwwastro.msfc.nasa.gov/lynx/.
26. J. W. Arenberg, "Analysis of the cost, schedule, and risk for Lynx mirror assembly production," Poster and Paper to be presented at *SPIE Opt. and Photonics 2019 Meeting*, San Diego, California, 11–15 August 2019 (in preparation).
27. J. W. Arenberg, "Formulation of the production time and cost of the Lynx mirror assembly based on queuing theory," *J. Astron. Telesc. Instrum. Syst.* **5**(2), 021016 (2019).
28. J. W. Arenberg, "Analysis of the Cost, Schedule and Risk for Lynx Mirror Assembly Production," Poster presented at the *AAS 17th Meeting, High Energy Astrophys. Div.*, Monterey, California, 17–21 March 2019 (in preparation).
29. R. A. Windhorst et al., "How JWST can measure first light, reionization and galaxy assembly," *New Astron. Rev.* **50**(1–3), 113–120 (2006).
30. R. C. Chase and L. P. Van Spreybroeck, "Wolter-Schwarzchild telescope for X-ray Astronomy," *Appl. Opt.* **12**(5), 1042–1044 (1973).
31. H. Wolter, "Generalized Schwarzschild mirror systems with glancing incidence on image producing optics for x-rays," *Ann. Phys.* **445**, 286–295 (1952).
32. A. Ernst, "On the estimation of aperture in the microscope," *J. R. Microsc. Soc.* **1**(3), 388–423, (1881).
33. B. Oppenheimer and J. Zuhone, "Elliptical galaxy data and simulations, the evolution and assembly of galaxies and their environments (EAGLE) project," http://icc.dur.ac.uk/Eagle/index.php (2019).
34. M. Weisskopf et al., "Chandra X-ray Observatory (CXO): overview," *Proc. SPIE* **4012**, 2–16 (2000).
35. Chandra X-ray Center, Chandra Project Science, MSFC, Chandra IPI Teams, "The Chandra Proposers' Observatory Guide," Version 21.0, http://cxc.harvard.edu/proposer/POG/pdf/MPOG.pdf (2018).
36. European Space Agency, "XMM-Newton Users Handbook and Science Analysis Software," https://www.cosmos.esa.int/web/xmm-newton/sas (2019).
37. European Space Agency, ATHENA Tools for Simulations, "Vignetting (as a function of off-axis angles at various energies)," https://www.cosmos.esa.int/web/athena/resources-by-esa (2019).
38. Y. Yao et al., "Progress of coating stress compensation of silicon mirrors for Lynx x-ray telescope mission concept using thermal oxide patterning method," *J. Astron. Telesc. Instrum. Syst.* **5**(2), 021011 (2019).
39. B. D. Chalifoux et al., "Simulations of film stress effects on mirror segments for the Lynx X-ray Observatory concept," *J. Astron. Telesc. Instrum. Syst.* **5**(2), 021004 (2019).

40. Private Communication with W. Zhang, NASA GSFC.
41. S. L. O'Dell et al., "X-ray optics at NASA Marshall Space Flight Center," *Proc. SPIE* **9510**, 951003 (2015).
42. R. Hudec, L. Pina, and A. Inneman, "Replicated x-ray optics for space applications," in *Int. Conf. Space Opt. ICSO 2000*, Toulouse, France (2000).
43. K. Kilaru et al., "Improving x-ray optics via differential deposition," *Proc. SPIE* **10399**, 103991F (2017).
44. M. Ghigo et al., "Final correction by ion beam figuring of thin shells for x-ray telescopes," *Proc. SPIE* **10706**, 107063I (2018).
45. J. Roche et al., "Active full-shell grazing-incidence optics," *Proc. SPIE* **9965**, 99650I (2016).
46. C. T. DeRoo et al., "Deterministic figure correction of piezoelectrically adjustable slumped glass optics," *Proc. SPIE* **10399**, 103991M (2017).
47. C. T. DeRoo et al., "Deterministic figure correction of piezoelectrically adjustable slumped glass optics," *J. Astron. Telesc. Instrum. Syst.* **4**(1) 019004 (2018).
48. V. Cotroneo et al., "Progress in development of adjustable optics for X-ray astronomy," *Proc. SPIE* **10761**, 1076109 (2018).
49. C. H. Kepner and B. B. Tregoe, *The Rational Manager*, McGraw-Hill, New York (1965).
50. G. Garmire et al., "Advanced CCD imaging spectrometer (ACIS) instrument on the Chandra X-ray Observatory," *Proc. SPIE* **4851**, 28–44 (2003).
51. M. J. L. Turner et al., "The European photon imaging camera on XMM-Newton: the MOS camera," *Astron. Astrophys.* **365**(1), L27–L35 (2001).
52. L. Strüder et al., "The European photon imaging camera on XMM-Newton: The pn-CCD Camera," *Astron. Astrophys.* **365**, L18–L26 (2001).
53. K. Koyama et al., "X-ray imaging spectrometer (XIS) on board Suzaku," *Publ. Astron. Soc. Jpn.* **59**(sp1), S23–S33 (2007).
54. N. Meidinger, K. Nandra, and M. Plattner, "Development of the wide field imager on ATHENA," *Proc. SPIE* **10699**, 106991F (2018).
55. European Space Agency, "XMM-Newton Science Archive," http://nxsa.esac.esa.int/nxsa-web/#home (25 April 2019).
56. F. B. S. Paerels and S. M. Kahn, "High-resolution x-ray spectroscopy with Chandra and XMM-Newton," *Annu. Rev. Astron. Astrophys.* **41**, 291–342 (2003).
57. J. Kaastra, "High-resolution x-ray spectroscopy: the coming-of-age," presented at *XMM-Newton: The Next Decade, Proc. Conf. held at ESAC*, 9–11 May, 2016, Madrid, id. 3, http://www.cosmos.esa.int/web/xmm-newton/2016-workshop (2016).
58. Hitomi Collaboration, "The quiescent intracluster medium in the core of the Perseus cluster," *Nature* **535**, 117–121 (2016)
59. D. Barret et al., "The ATHENA x-ray integral field unit (X-IFU)," *Proc. SPIE* **10699**, 106991G (2018).
60. B. D. Jackson et al., "The focal plane assembly for the ATHENA x-ray integral field unit instrument," *Proc. SPIE* **9905**, 99052I (2016)
61. D. Barret et al., "The ATHENA x-ray integral field unit (X-IFU)," *Proc. SPIE* **9905**, 99052F (2016).
62. C. P. de Vries et al., "Calibration sources and filters of the soft x-ray spectrometer instrument on the Hitomi spacecraft," *J. Astron. Telesc. Instrum. Syst.* **4**(1), 011204 (2017)
63. C. P. de Vries et al., "Filters and calibration sources for the soft x-ray spectrometer (SXS) instrument on ASTRO-H," *Proc. SPIE* **7732**, 773213 (2010)

Jessica A. Gaskin received her BS degree in physics (astrophysics) from New Mexico Tech., followed by her MS degree in astronomy from the Case Western University, and her PhD in physics from University of Alabama in Huntsville. She has been a NASA civil servant for 15 years in the X-Ray Astronomy Group at Marshall Space Flight Center. She is the NASA-appointed study scientist for the Lynx X-ray Observatory concept study, which is one of the four candidate missions up for prioritization in the 2020 Astrophysics Decadal Survey. Her background is in the development and testing of optics and instrumentation for high-energy astrophysics and planetary science.

Biographies of the other authors are not available.